Journal of Organometallic Chemistry, 440 (1992) 27–40
Elsevier Sequoia S.A., Lausanne
JOM 22888

Mössbauer and NMR study of tin(IV) and organotin(IV) hydridotris(3-Me-1*H*-pyrazol-1-yl)borates. The X-ray crystal structure of phenyldichlorotin(IV) derivative

Giancarlo Gioia Lobbia
Dipartimento di Scienze Chimiche, Università di Camerino, Via S. Agostino 1, I-62032 Camerino (Italy)

Sandro Calogero
Dipartimento di Chimica Fisica, Università di Venezia, I-30123 Venezia (Italy)

Bruna Bovio
Dipartimento di Chimica Generale, viale Taramelli 12, I-27100 Pavia (Italy)

and Patrizio Cecchi
Dipartimento di Agrobiologia ed Agrochimica, Università della Tuscia, Via S.C. De Lellis, I-01100 Viterbo (Italy)

(Received March 3, 1992)

Abstract

Tin(IV) and organotin(IV) compounds containing the hydridotris(3-methyl-1*H*-pyrazol-1-yl)borate ligand (L^1) $R_nSnCl_{4-n-1}\cdot L^1$ (R = Me, Et, Bu, CH_2=CH, or Ph; $n = 0$–2) have been synthesized and studied by ^{119m}Sn Mössbauer and NMR (^{1}H, ^{13}C, ^{119}Sn) spectroscopic techniques. The compounds are not fluxional and contain six-coordinate tin(IV) with a tridentate ligand, *i.e.* $(R_nCl_{4-n-1})Sn(\mu\text{-pz-}N,N')_3BH$ (pz = 3-Me-pyrazolato group). X-Ray single crystal analysis of $PhCl_2Sn[HB(3\text{-Me-Pz})_3]$ is reported. Six-coordinate tin is present in a distorted octahedron; the octahedron axes are not orthogonal (angles 167.7(2), 167.8(1) and 174.0(3)°). The Sn–C bond (2.23(1) Å) is long; the Sn–N bonds (2.218(6), 2.241(6), 2.289(5) Å) and Sn–Cl bonds (2.420(2), 2.438(2) Å) are normal. The ^{119m}Sn Mössbauer parameters at 4.2 K of the compounds are reported and discussed.

Introduction

Research on the coordination chemistry of polypyrazolylborate has developed very rapidly in recent years [1]. Notwithstanding that some twenty five years have been elapsed since they were introduced by Trofimenko, their peculiar feature of being flexible anionic bi- or tri-dentate ligands is still prompting interest in the

---

Correspondence to: Professor G. Gioia Lobbia.

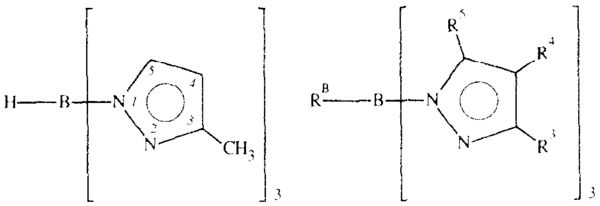

	R^B	R^3	R^4	R^5
L^0	–	–	–	–
→ L^1	–	Me	–	–
L^2	–	Me	–	Me
L^3	–	Me	Me	Me
L^B	Pz*	–	–	–

(*) Pz = 1*H*-pyrazol-1-yl

Fig. 1. Hydridotris(3-Me-1*H*-pyrazol-1-yl)borate (L^1), together with the ring numbering scheme, related to other polypyrazolylborate-ligands. Pz = 1*H*-pyrazol-1-yl.

coordination chemistry of transition- and especially post-transition (organo)metal cations [2].

In a preceding paper [3a] the interaction of potassium hydridotris(3,5-dimethyl)pyrazolylborate (Fig. 1) KL^2 and organotin(IV)halides ($R_nSn(Hal)_{4-n}$ (R = alkyl or aryl; $n = 0$, 1 or 2) was examined. Six-coordinate and non-fluxional complexes $R_nSn(Hal)_{4-n-1} \cdot L^2$ with L^2 tridentate were found. L^2 (and the less common L^3) is undoubtedly a better donor to the proton than the unsubstituted L^0, but may be worse with a metal to which close approach is prevented by steric hindrance. Linear correlations were found between the ^{119}Sn chemical shift of the complexes and the number of halogen atoms attached to the tin(IV) centre for L^0, L^B, L^2, and for R = Me, ^nBu, or Ph [3]. Although the shifts relevant to the complexes of L^B and L^0 are almost superimposable, those from L^2, although falling on a parallel line, are displaced from it, indicating different behaviour. In order to gain a further insight into the coordination chemistry of organotin(IV) halides, it was decided to investigate complexes of L^1 which has a steric demand towards tin like that of the 3,5-dimethylsubstituted species but is a poorer donor.

Results and discussion

The compounds listed in Table 1 were obtained as white solids which gave satisfactory elemental analyses in fair-to-good yields from interaction of KL^1 and the appropriate organotin halide in dichloromethane solution/suspension. Molecular weight determinations by osmometry showed them to be monomeric in dichloromethane and non-electrolytes in acetone solution (Table 1), like the corresponding compounds containing L^0, L^2, or L^B [3].

IR spectra (Table 2) show that ν (B–H) is sensitive to structure: the greater the number of tin-bonded chlorine atoms, the higher the frequency.

The ^1H (Table 3) and ^{13}C (Table 4) NMR spectra support the proposed formulae. The assignment of the H and C signals from the 3-, 4-, and 5-position of

Table 1

Yields, analyses, and physical properties of compounds

	Compound	Yield	Elemental analysis (Found (calcd.)) (%)			M.p. (°C)	A [b]
			C	H	N		
1	$SnCl_3\cdot L^1$ [a]	78	29.88	3.40	17.29	> 300 [c]	4.5
			(30.02)	(3.36)	(17.50)		(0.9)
2	$CH_3SnCl_2\cdot L^1$ [a]	74	33.64	4.30	17.92	237–239	7.5
			(33.96)	(4.17)	(18.28)		(1.1)
3	$C_4H_9SnCl_2\cdot L^1$	69	38.14	5.09	16.64	176–177	3.1
			(38.30)	(5.02)	(16.75)		(1.0)
4	$C_6H_5SnCl_2\cdot L^1$	86	41.33	4.09	15.96	212–214	5.5
			(41.43)	(4.06)	(16.11)		(0.9)
5	$(CH_3)_2SnCl\cdot L^1$ [a]	68	38.02	5.12	19.00	147–149	8.9
			(38.28)	(5.05)	(19.13)		(1.0)
6	$(C_2H_5)_2SnCl\cdot L^1$	58	41.02	5.65	17.77	108–110	8.2
			(41.12)	(5.61)	(17.98)		(1.0)
7	$(C_4H_9)_2SnCl\cdot L^1$	46	45.98	6.61	15.93	[c]	10.2
			(45.89)	(6.55)	(15.93)		(1.0)
8	$(C_6H_5)_2SnCl\cdot L^1$ [a]	77	51.08	4.55	14.69	267–269	7.5
			(51.16)	(4.65)	(14.91)		(1.0)
9	$(CH_2{=}CH_2)_2SnCl\cdot L^1$	46	41.11	4.88	17.94	163–165	12.8
			(41.48)	(4.79)	(18.14)		(0.9)

[a] Monomeric according to molecular weight determination by osmometry in dichloromethane. [b] Specific conductivity (ohm^{-1}cm^{2}mol^{-1}) in acetone solution at room temperature and the molar concentration $\times 10^{-3}$ indicated in parentheses in the lower line. [c] Chars without melting.

Table 2

IR data

Compound	Pyrazole C–H stretching	B–H	ring breathing	< 500	Others
$K\cdot L^1$	3115 w, sh; 3106 w; 3095 w, sh	2400 m	1507 s	405 m; 340 w	
1	3110 w, sh 3104 m	2555 m	1505 s	370 m; 410 m; 430 w	ν(Sn–Cl) 290 m 310 s, br
2	3115 w, sh 3105 w	2510 m	1504 s	415 m;	ν(Sn–Cl) 290 s, br
3	3132 w, sh 3110 m	2518 m	1505 s	340 w; 360 w; 410 m	ν(Sn–Cl) 285 s, br
4	3095 w 3106 w	2529 m	1501 s	352 w; 410 w 465 m	ν(Sn–Cl) 280 m, br
5	3121 w, sh 3101 w	2478 m	1505 m	340 w 405 m	ν(Sn–Cl) 280 m
6	3104 w, sh 3097 w	2496 m	1509 s	350 w; 390 w 410 m; 430 w	ν(Sn–Cl) 285 m
7	3118 w, sh 3110 w	2498 m	1505 m	340 w, 390 w 415 m	ν(Sn–Cl) 295 m
8	3110 w	2484 m	1506 m	340 w; 405 m; 490 w	ν(Sn–Cl) 280 s
9	3126 w, sh 3115 w	2498 m	1500 s	340 w; 410 m 455 w; 470 m	ν(Sn–Cl) 290 m

Table 3

^{1}H NMR data

No.	Compound	Solvent	5–H (doublets) $\delta^{a,b}$	4–H $\delta^{a,b}$	3–Me $\delta^{a,b}$	Sn–R, ^nJ(Sn–H)/Hz ^{c}, and notes
	KL^1	$(CD_3)_2CO$	7.42	5.75	2.13	
		$CDCl_3$	7.48	6.06	2.31	
		$CDCl_3$^{d}	7.00	5.82	2.22	
1	$SnCl_3 \cdot L^1$	$CDCl_3$	8.12	6.17	2.45	
2	$MeSnCl_2 \cdot L^1$	$CDCl_3$	7.55	6.05	2.62	Me: 1.57; $^2J = 119$
			7.49	6.08	2.88	
3	$BuSnCl_2 \cdot L^1$	$CDCl_3$	7.57	6.10	2.62	Bu: 2.05–1.94 m; 1.78–1.65 m;
			748 *	6.02 *	2.87	1.42 sextet; 0.92 t; (*) $^{3,4}J \approx 14$
4	$PhSnCl_2 \cdot L^1$	$CDCl_3$	7.62	6.00	1.93	Ph: 7.26–7.32 m; 7.40–7.48 m;
			7.56	6.10	2.94	7.52–7.60 m
5	$Me_2SnCl \cdot L^1$	$CDCl_3$	7.48	5.96	2.40	Me: 1.02; $^2J = 67$
			7.60	6.07	2.61	
6	$Et_2SnCl \cdot L^1$	$CDCl_3$	7.65	6.12	2.38	Et: 1.44 t; 1.75 q; ^3J(H–H) = 7
			7.58	6.00	2.60	
7	$Bu_2SnCl \cdot L^1$	CD_2Cl_2	7.45	6.15	2.36	Bu: 1.84–1.80 m; 1.54–1.26 m;
			7.52	6.06	2.30	0.94 t;
8	$Ph_2SnCl \cdot L^1$	$CDCl_3$	7.56	5.91 *	1.89	Ph: 7.52–7.56 m; 7.42–7.48 m;
			7.74	6.00	1.32	7.20–7.30 m; (*) $^4J \approx 21$
9	$Vi_2SnCl \cdot L^1$	$CDCl_3$	7.46	5.95	2.58	Vi: 6.72 dd; 6.1 dd; 5.9 dd
			7.58	5.86	2.24	$^2J = 168$; $^3J_{cis}$(H–H) = 13.6 $^3J_{trans}$(H–H) = 20.0

[a] In the compounds **2–9** the upper line signals have twice the intensity of those in the lower lines. [b] In ppm from internal Me_4Si. [c] Except when otherwise stated. [d] In the presence of an equivalent of 18-Crown-6.

the pyrazole ring is easier than with compounds of L^0 or L^2. The ^{13}C resonances between 105 and 107 ppm can clearly be assigned to the carbon atoms in the 4-position. The other signals of the pyrazole rings appear between 135 and 140 ppm for 5-C, and between 148 and 156 ppm for 3-C, the latter being much less intense owing to the lack of a hydrogen atom. For compounds with $n \neq 0$, two sets of signals from every ring position (methyl groups included) are observable in both ^{1}H (in 2 : 1 integration ratio) and ^{13}C spectra (one set more intense than the other). This is consistent with octahedral coordination geometry and with the corresponding compounds containing L^B, L^0, and L^2.

These observations clearly rule out fluxionality [3] around the tin(IV) in solution at room temperature. Of the two 2 : 1 signals (^{1}H spectra) from the three 3-methyl groups, the more intense in **4** ($PhSnCl_2 \cdot L^1$) and the less intense in **9** ($Ph_2SnCl \cdot L^1$) appear abnormally shielded. Assuming the structure of **4** in solution is similar to its crystal structure (Fig. 2), this is readily explained by the anisotropy of the phenyl ring shielding: in **4** the phenyl ring lies between two Me groups. If allowance is made for replacement in the structure of **4** of a chorine atom with a phenyl ring in a similar orientation then one Me group in **9** should face two phenyl rings almost face-on, and each of them would face one of the other two Me groups. These influences are less reflected even in 4-H resonance positions. Often a 3-pyrazole

Table 4

^{13}C and ^{119}Sn NMR data

No.	Compound	Solvent	3-C δ [a,b]	5-C δ [a,b]	4-C δ [a,b]	Pz-CH_3 δ [a,b]	Sn-R, ^nJ(Sn-C)/Hz, and notes	^{119}Sn $-\delta$ [c]
	K·L^1	$(CD_3)_2CO$	147.7	135.6	102.6	13.7		
1	$SnCl_3 \cdot L^1$	$CDCl_3$	153.2	140.1	106.6	12.1		651
2	$MeSnCl_2 \cdot L^1$	$CDCl_3$	151.2	135.7	106.7	13.9	Me: 29.7	506
			152.8	135.5	107.3	15.4		
3	$BuSnCl_2 \cdot L^1$	$CDCl_3$	151.3	135.9	106.7	14.0	Bu: 41.9; 27.1;	503
			153.1	135.7	107.2 *	15.4	25.8; 13.7	
							$^1J = 1138$, $^2J = 261$,	
							$^3J \approx 67$; (*) $^3J \approx 37$	
4	$PhSnCl_2 \cdot L^1$	$CDCl_3$	152.7	135.9	106.6	13.6	Ph: 136.2; 132.0	552
			153.4	135.8	107.3	15.3	128.2; 127.0	
5	$Me_2SnCl \cdot L^1$	$CDCl_3$	150.2	138.8	105.6	12.2	Me: 19.0; $^1J = 655$	353
			149.1	136.2	105.0	14.3		
6	$Et_2SnCl \cdot L^1$	$CDCl_3$	151.3	136.2	105.4	12.3	Et: 9.4; 23.9	330
			149.8	[d]	106.1	11.8		
7	$Bu_2SnCl \cdot L^1$	$CDCl_3$	[d]	135.0	104.4	11.7	Bu: 32.7; 27.2;	337
				143.0	106.2	12.1	26.3; 13.4	
8	$Ph_2SnCl \cdot L^1$	$CDCl_3$	156.2	136.0	106.1	13.7	Ph: 140.2; 135.0;	476
			152.1	134.9	105.9	13.5	128.2; 127.4	
9	$Vi_2SnCl \cdot L^1$	$CDCl_3$	151.4	134.8	106.0	14.7	Vi: 154.7 *; 130.7	489
			153.7	135.7	105.5	13.8	(*) $^1J = 897$	

[a] The upper line signals in **2–9** are more intense than those on the lower lines. [b] In ppm from internal Me_4Si. [c] In ppm from external Me_4Sn. [d] Not observed.

carbon *trans* to an alkyl or aryl carbon atom exhibits a higher chemical shift than that *trans* to a chlorine atom. This is found in all compounds **2–9**, and may be an expression of electronic orbital population imbalance evident from the Mössbauer spectra of the same compounds.

In the spectra of some compounds especially the R_2SnCl derivatives minor peaks are seen. The overall intensity may reach one sixth of the main peaks. This may be due to an inversion of one or more 3-methylpyrazolato groups which then

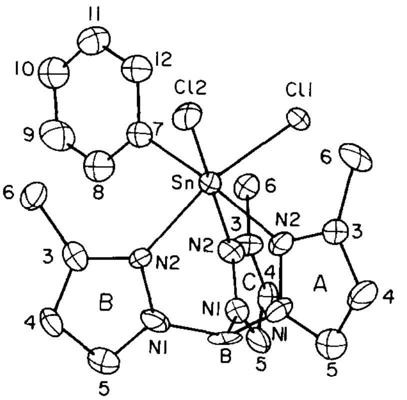

Fig. 2. ORTEP plot and numbering scheme. Thermal ellipsoids enclose 25% of the electron density. Hydrogen atoms are omitted for clarity.

Table 5

Crystal data, data collection, and refinement of the structure

Formula	$C_{18}H_{21}BCl_2N_6Sn$
Formula weight	521.8
Space group	$C2/c$
Colour	colourless
a, Å	25.947(5)
b, Å	10.366(2)
c, Å	16.337(7)
β, deg	94.77(2)
V_c, Å^3	4379(2)
Z	8
D_{calcd}, gcm^{-3}	1.58
Cryst. size, mm	0.10 × 0.28 × 0.28
μ (Mo-K_α), cm^{-1}	14.33
Data collection instrument	Enraf–Nonius CAD4
Radiation (monochromated)	Mo-K_α($\lambda = 0.7107$ Å)
T of data collection, K	293
Scan mode	$\omega/2\vartheta$
Data collection range	$2 < \vartheta < 30°$
Stds (measured every 300 min)	$-4\ -2\ 4$, $-4\ -2\ 1$, $-7\ -1\ 0$
No. of unique reflns.	4679 (h, k, $\pm l$)
No. of data with $F_0^2 > 3\sigma(F_0^2)$	3723
No. of parameter refined	253
R [a] and R_w [b]	0.054, 0.068

[a] $R = \{\Sigma \| F_o| - k|F_c\|\}/\Sigma|F_o|$. [b] $R_w = [\Sigma w(|F_o| - k|F_c|)^2/\Sigma w|F_o|^2]^{1/2}$.

become 5-methyl. This has been observed for more sterically demanding ligands, hydridotris(3-i-propyl-1*H*-pyrazolyl)borate and its 4-Br analogue. The crystal structures of their Co^{II} derivatives show a rearrangement of one pyrazole moiety [2f]. It is our aim to investigate this phenomenon further.

X-Ray crystal structure of $PhSnCl_2 \cdot L^1$

The crystal structure of [hydrotris(3-methyl-1*H*-pyrazol-1-yl)borate]phenyldichlorotin(IV) **4** consists of discrete monomeric molecules. An ORTEP view [4] is shown in Fig. 2, along with its numbering scheme. The molecule exhibits no real symmetry and all atoms occupy general positions though virtual C_s symmetry with the mirror plane coinciding with the ring planes N(1A)–C(5A) and C(7)–C(12) and passing through Sn and B can be identified. Crystallographic data, bond distances and angles, and final atomic coordinates are reported in Tables 5, 6, and 7.

The displacements of atoms from the least-squares planes of the pyrazole and phenyl rings are small so that these moieties may be considered planar.

The shortest intermolecular approaches between the molecules are normal van der Waals contacts.

The tin(IV) atom has distorted octahedral coordination; the *cis*-angles range from 81.4(2) to 97.2(4)° and the *trans*-angles from 167.7(2) to 174.0(3)°.

The hydridotris(3-methyl-1*H*-pyrazol-1-yl)borate moiety is a facial tridentate ligand, with "bite" angles (*ca.* 81.6°), markedly less than 90°. The C(7)–Sn–N(2A) axis is bent (174.0(3)°) so that the N(2A) atom leans towards the midpoint of the segment N(2B) · · · N(2C), but the phenyl group is bigger and thus the four

Table 6

Interatomic distances (Å) and bond angles (deg) (with esd's in parentheses). Data for the coordination sphere are listed in Table 8, under column *a* *

In the ligands			
N(1A)-B	1.56(1)	N(1C)-B	1.505(8)
N(1A)-N(2A)	1.368(8)	N(1C)-N(2C)	1.338(9)
N(2A)-C(3A)	1.328(8)	N(2C)-C(3C)	1.351(8)
C(3A)-C(4A)	1.42(1)	C(3C)-C(4C)	1.39(1)
C(3A)-C(6A)	1.55(1)	C(3C)-C(6C)	1.54(1)
C(4A)-C(5A)	1.34(1)	C(4C)-C(5C)	1.38(1)
C(5A)-N(1A)	1.39(1)	C(5C)-N(1C)	1.34(1)
N(1B)-B	1.52(1)	C(7)-C(8)	1.38(2)
N(1B)-N(2B)	1.333(8)	C(8)-C(9)	1.40(2)
N(2B)-C(3B)	1.35(1)	C(9)-C(10)	1.38(2)
C(3B)-C(4B)	1.39(1)	C(10)-C(11)	1.39(2)
C(3B)-C(6B)	1.54(1)	C(11)-C(12)	1.39(2)
C(4B)-C(5B)	1.36(1)	C(12)-C(7)	1.38(2)
C(5B)-N(1B)	1.36(1)	C(4B)-C(3B)-C(6B)	125.9(8)
N(1A)-B-N(1B)	113.0(5)	C(3B)-C(4B)-C(5B)	106.9(7)
N(1A)-B-N(1C)	107.0(6)	C(4B)-C(5B)-N(1B)	106.5(7)
N(1B)-B-N(1C)	108.8(6)	N(2C)-N(1C)-C(5C)	112.2(6)
N(2A)-N(1A)-C(5A)	108.8(6)	N(2C)-N(1C)-B	119.6(5)
N(2A)-N(1A)-B	120.6(6)	C(5C)-N(1C)-B	128.0(7)
C(5A)-N(1A)-B	130.6(6)	N(1C)-N(2C)-C(3C)	105.8(5)
N(1A)-N(2A)-C(3A)	109.2(6)	N(1C)-N(2C)-Sn	121.7(4)
N(1A)-N(2A)-Sn	117.8(4)	C(3C)-N(2C)-Sn	131.9(5)
C(3A)-N(2A)-Sn	132.9(5)	N(2C)-C(3C)-C(4C)	109.6(6)
N(2A)-C(3A)-C(4A)	105.9(7)	N(2C)-C(3C)-C(6C)	125.5(7)
N(2A)-C(3A)-C(6A)	124.3(6)	C(4C)-C(3C)-C(6C)	124.9(7)
C(4A)-C(3A)-C(6A)	129.6(7)	C(3C)-C(4C)-C(5C)	105.8(7)
C(3A)-C(4A)-C(5A)	109.7(9)	C(4C)-C(5C)-N(1C)	106.6(8)
C(4A)-C(5A)-N(1A)	105.8(8)	C(8)-C(7)-C(12)	120(1)
N(2B)-N(1B)-C(5B)	110.6(7)	C(8)-C(7)-Sn	122(1)
N(2B)-N(1B)-B	120.2(6)	C(12)-C(7)-Sn	118(1)
C(5B)-N(1B)-B	125.3(5)	C(7)-C(8)-C(9)	120(1)
N(1B)-N(2B)-C(3B)	107.2(6)	C(8)-C(9)-C(10)	120(1)
N(1B)-N(2B)-Sn	120.3(5)	C(9)-C(10)-C(11)	120(1)
C(3B)-N(2B)-Sn	132.2(5)	C(10)-C(11)-C(12)	120(1)
N(2B)-C(3B)-C(4B)	108.6(7)	C(11)-C(12)-C(7)	120(1)
N(2B)-C(3B)-C(6B)	125.4(7)		

cis-angles concerning C(7) are greater than 90° and the Sn–C(7) bond (2.228(14) Å) is longer than a normal Sn–C bond (2.10–2.19 Å) owing to the steric demand of the tridentate ligand. The Sn–C bond lengths in *trans*-$[Me_2Sn(acac)_2]$ (2.14(2) Å) [5], *trans*-$[Bu_2Sn(dbm)_2]$ (2.115(10) Å) [6], *trans*-$[Bu_2Sn(PhMeBenzoylpyrazolonate)_2]$ (2.204(11), 2.196(17) Å) [7], $[HB(pz)_3SnMe_3]$ (2.165(2) Å) [8], $[HB(pz)_3Sn(CH_2CH_2COOMe)Cl_2]$ (2.140(7) Å) [9] and $HB(pz)_3Sn(CH_2CH_2COOMe)(NCS)_2$ (2.124(5) Å) [9] are shorter than in compound **4**.

The Cl(1)–Sn–N(2B) and Cl(2)–Sn–N(2C) angles are 167.8(1) and 167.7(2)° respectively so as to keep the ligands away from the phenyl group. The Sn–Cl bonds (2.420(2), 2.438(2) Å) are longer than in $SnCl_2[ONPh(COPh)]_2$ (2.366(5), 2.356(6) Å) [10] and $SnCl_2[PhCOCHCOPh]_2$ (2.335(2), 2.344(2) Å) [11], but similar

Table 7

Final coordinates and equivalent isotropic thermal parameters (with esd's in parentheses)

Atom	*x*	*y*	*z*	*B* (Å^2)
Non-hydrogen atoms				
Sn	0.12590(2)	0.32673(5)	0.13666(3)	2.801(4)
Cl(1)	0.0770(1)	0.4712(2)	0.2171(1)	4.15(3)
Cl(2)	0.2052(1)	0.3498(2)	0.2265(1)	4.47(4)
B	0.1279(2)	0.3750(9)	−0.0627(3)	3.3(1)
N(1A)	0.1473(3)	0.4996(7)	−0.0167(3)	3.8(1)
N(2A)	0.1517(2)	0.5041(4)	0.0672(3)	2.94(7)
C(3A)	0.1684(3)	0.6201(6)	0.0916(4)	3.6(1)
C(4A)	0.1783(6)	0.6876(8)	0.0192(7)	5.4(2)
C(5A)	0.1616(3)	0.6181(7)	−0.0467(5)	5.6(2)
C(6A)	0.1781(4)	0.6619(6)	0.1825(5)	6.0(1)
N(1B)	0.1601(3)	0.2565(8)	−0.0373(3)	3.58(9)
N(2B)	0.1688(3)	0.2257(5)	0.0418(3)	3.55(9)
C(3B)	0.2015(2)	0.1247(8)	0.0464(5)	3.7(1)
C(4B)	0.2135(3)	0.0933(8)	−0.0325(5)	4.2(1)
C(5B)	0.1887(2)	0.1807(9)	−0.0843(4)	3.9(1)
C(6B)	0.2195(4)	0.0508(10)	0.1255(7)	4.8(2)
N(1C)	0.0731(2)	0.3528(6)	−0.0423(4)	3.32(9)
N(2C)	0.0636(2)	0.3258(6)	0.0351(4)	4.22(7)
C(3C)	0.0116(2)	0.3186(8)	0.0348(4)	3.91(9)
C(4C)	−0.0109(3)	0.3478(6)	−0.0432(8)	4.4(1)
C(5C)	0.0297(4)	0.3657(10)	−0.0917(6)	4.6(1)
C(6C)	−0.0185(3)	0.2871(12)	0.1099(8)	4.6(1)
C(7)	0.1008(6)	0.1429(13)	0.1919(7)	11.8(6)
C(8)	0.0859(6)	0.0368(15)	0.1447(11)	11.9(9)
C(9)	0.0730(6)	−0.0790(15)	0.1820(11)	9.1(6)
C(10)	0.0775(7)	−0.0884(14)	0.2667(9)	11.6(7)
C(11)	0.0925(6)	0.0186(14)	0.3143(8)	7.6(5)
C(12)	0.1053(6)	0.1335(12)	0.2766(12)	9.0(8)

to those in $SnCl_2(btbm)_2$ (2.414(2), 2.410(3) Å) [12], $SnCl_2(tacac)_2$ (2.416(1) Å) [12], $SnCl_2[SCH_2CH(NH_2)COOMe]_2$ (2.445(3), 2.445(3) Å) [13] and $HB(pz)_3Sn(CH_2CH_2COOMe)Cl_2$ (2.413(2), 2.442(2) Å) [9].

In our compound, the Cl–Sn–Cl angle (93.81(8)°) is in the range 82.0–94.5° and the non-bonding Cl · · · Cl distance (3.548(3) Å) is less than 3.6 Å, features suggested by Koepf *et al.* [14] as a criterion of anti-tumour activity in metallocene dichlorides.

The Sn–N bonds (2.218(6), 2.241(6), 2.289(5) Å), slightly larger than the sum of covalent radii (2.10 Å), are shorter than in $HB(pz)_3SnMe_3$ (2.388(2) Å) [8] and $SnCl_2[SCH_2CH(NH_2)COOMe]_2$ (2.264(10), 2.309(10) Å) [13] and comparable with those in $[HB(pz)_3Sn(CH_2CH_2COOMe)Cl_2]$ (2.225(7), 2.237(6), 2.191(7) Å) and in $[HB(pz)_3Sn(CH_2CH_2)COOMe)(NCS)_2]$ (2.219(4), 2.239(4), 2.197(4) Å) [9].

Of the three pyrazole rings, those *trans* to chlorides have similar dimensions to those of the pyrazole in $HB(pz)_3SnMe_3$ [8] but the third is different. This may arise from the greater *trans*-influence of Ph compared with that of Cl.

Bond distances and angles in the title compound and in related tin(trispyrazolylborato) compounds are given in Table 8, in which a common numbering system is used.

Table 8

Comparison of some structural data

Compound	*a* *	*b* [9]	*c* [9]	*d* [8]	*e* [15]	*f* [15]
Distances (Å)						
Sn–N(2A)	2.289(5)	2.191(7)	2.197(4)	2.388(2)	2.361(2)	2.214(3)
Sn–N(2B)	2.241(6)	2.237(6)	2.239(4)	2.388(2)	2.510(2)	2.491(2)
Sn–N(2C)	2.218(6)	2.225(7)	2.219(4)	2.388(2)	2.462(2)	2.215(3)
Sn–C(7)	2.228(14)	2.140(7)	2.124(5)	2.165(2)		
Sn–Cl(1)	2.420(2)	2.413(2)				2.629(1)
Sn–Cl(2)	2.438(2)	2.442(2)				
Angles (deg)						
N(2A)–Sn–N(2B)	81.4(2)	79.0(2)	81.1(1)	74.8(1)	76.50(7)	76.99(9)
N(2A)–Sn–N(2C)	81.8(2)	81.5(2)	80.7(2)	74.8(1)	74.84(8)	84.3(1)
N(2B)–Sn–N(2C)	81.6(2)	80.4(3)	81.5(1)	74.8(1)	82.22(7)	76.56(9)
N(2A)–Sn–C(7)	174.0(3)	171.4(3)	172.5(2)	157.9(1)		
N(2B)–Sn–C(7)	93.4(4)	93.2(3)	91.9(2)	86.8(1)		
N(2C)–Sn–C(7)	94.6(4)	95.0(3)	100.9(2)	88.8(1)		
Cl(1)–Sn–N(2A)	87.7(1)	88.1(2)				85.94(7)
Cl(1)–Sn–N(2B)	167.8(1)	166.4(2)				156.91(7)
Cl(1)–Sn–N(2C)	91.5(2)	92.3(2)				86.48(7)
Cl(1)–Sn–C(7)	97.2(4)	99.4(2)				
Cl(1)–Sn–Cl(2)	93.81(8)	94.3(1)				
Cl(2)–Sn–N(2A)	87.3(2)	87.4(2)				
Cl(2)–Sn–N(2B)	91.1(2)	89.3(2)				
Cl(2)–Sn–N(2C)	167.7(2)	165.9(2)				
Cl(2)–Sn–C(7)	95.8(4)	96.2(2)				

[a] $HB(3\text{-}Mepz)_3Sn(C_6H_5)Cl_2$. [b] $HB(pz)_3Sn(CH_2CH_2COOCH_3)Cl_2$. [c] $HB(pz)_3Sn(CH_2CH_2COOCH_3)(NCS)_2$. [d] $HB(pz)_3Sn(CH_3)_3$. [e] $[HB(3,5\text{-}Me_2pz)_3]_2Sn$. [f] $HB(3,5\text{-}Me_2pz)_3SnCl$. * : present study.

The data of $[HB(3,5\text{-}Me_2pz)_3]_2Sn$ are exceptional [15], owing to the Sn^{II} active lone-pair, whereas the data of $HB(pz)_3Sn(CH_2CH_2COOMe)Cl_2$ [9] and $HB(pz)_3Sn(CH_2CH_2COOMe)(NCS)_2$ [9] are much more similar.

The steric demands of ligands are important in determining the stability of metal complexes, in ligand competition, and in ligand exchange. It is of value to calculate effective cone angles of ligands from the established crystallographic structural data. In our complex the three 3-Me-pyrazolyl groups lie in positions without threefold symmetry. The middle of the three Sn–N vectors is assumed to be cone axis and the cone vertex is centred on the tin atom: the angle between the cone axis and the vector which touches the van der Waals radii of the methyl hydrogen atoms closest to Sn ($r = 1.17$ Å for H) for each end of the tridentate ligand is 118.3° for H(6A1), 118.6° for H(6B1) and 119.9° for H(6C2). These angles correspond to a total average value (similar to that for an unsymmetrical ligand) of 237.8°, which is notably larger than the value 224° estimated by Trofimenko *et al.* [16] for L^1.

Mössbauer spectra

The isomer shifts, quadrupole splitting and average linewidth at half-maximum are reported in Table 9. The linear relationship between quadrupole splitting and

Table 9

^{119m}Sn Mössbauer parameters at 4.2 K

	Compound [a]	Isomer shift [b]	Quadrupole splitting obs.	Quadrupole splitting calc.	Average line-width at half-maximum
1	$SnCl_3 \cdot L^1$	0.24(1)	–	0.00 [c]	0.90(1)
2	$CH_3SnCl_2 \cdot L^1$	0.72(1)	1.73(1)	+2.06 [c]	0.83(1)
4	$PhSnCl_2 \cdot L^1$	0.67(1)	1.52(1)	+1.90 [c]	0.83(1)
5	$(CH_3)_2SnCl \cdot L^1$	0.88(1)	2.26(1)	−2.06 [c]	0.84(1)
8	$Ph_2SnCl \cdot L^1$	0.83(1)	2.13(1)	−1.90 [c]	0.85(1)
9	$(CH_2{=}CH)_2SnCl \cdot L^1$	0.78(1)	1.99(1)	−2.06 [c]	0.90(1)
		1.30(1)	3.75(2)		0.80(1) 24% [d]

[a] Three compounds referred to in the previous tables are not included here: their Mössbauer parameters are expected to be very similar to those reported in this table for **2** (compound **3**) and for **5** (compounds **6** and **7**). [b] Relative to SnO_2. [c] Calculated by using the point-charge model and the literature [18a] octahedral partial quadrupole splittings, in mm/s. Cl = 0.00, Me = −1.03, Ph = −0.95. As previously reported [18b] the partial quadrupole splitting for Me has been assumed as a working approximation for vinyl. [d] Percentage of the tin site calculated by Mössbauer resonance area.

isomer shift values for the compounds **2**, **4**, **5**, **8**, and **9** shows that the tin coordination number is greater than four [17].

All the Mössbauer spectra are quadrupole doublets, except that of compound **1** which shows a single line and the vinyl derivative **9** with two doublets (Fig. 3).

The point-charge model [18] has been used to calculate the observed electric quadrupole interactions employing the literature partial quadrupole splitting figures (Table 9).

In a regular octahedral geometry with a facial *N*-tridentate ligand, the $(3\text{-Me-Pz})_3BH^-$ (L^1) ligand does not contribute to the expression of the principal components V_{xx}, V_{yy}, and V_{zz} of the electric field gradient tensor. For $SnCl_3 \cdot L^1$ (**1**), where C_{3v} microsymmetry is present in the octahedral geometry, neither L^1 nor the three facial Cl ligands contribute to the latter tensor so that $V_{xx} = V_{yy} = V_{zz} = 0$. The unresolved quadrupole splitting is therefore consistent with C_{3v} octahedral symmetry for the tin.

Within the limits of the point-charge model the agreement between observed and calculated quadrupole splitting values in Table 9 is good, assuming octahedral geometry for $RSnCl_2 \cdot L^1$ (**2**, **4**) and $R_2SnCl \cdot L^1$ (**5**, **8** and first site of **9**). From this assignment the principal components for the compound $RSnCl_2 \cdot L^1$ are equal in magnitude but opposite in sign to those of the compounds $R_2SnCl \cdot L^1$.

The sign of V_{zz} in complexes where the electric field gradient tensor is not zero may be deduced by considerations of the relative electron donor power of the ligands at the tin site. In the derivatives **2** and **4** more negative charge is concentrated along the R–Sn–N axis in comparison with the equally populated p_x and p_y orbitals, giving a negative V_{zz}.

In the compounds **5**, **8**, and in the first site of **9**, more negative charge is concentrated along the R–Sn–N axes, giving a positive V_{zz}. Because the ^{119m}Sn nuclear quadrupole moment is negative [19], the quadrupole splitting values are positive for the adducts **2** and **4** and negative for **5**, **8** and the first site of **9**, in agreement with the point-charge model (Table 9 and Fig. 3).

The second doublet in the Mössbauer spectrum of compound **9** may be due to the partial air alteration characteristic of the of dialkyltin compounds.

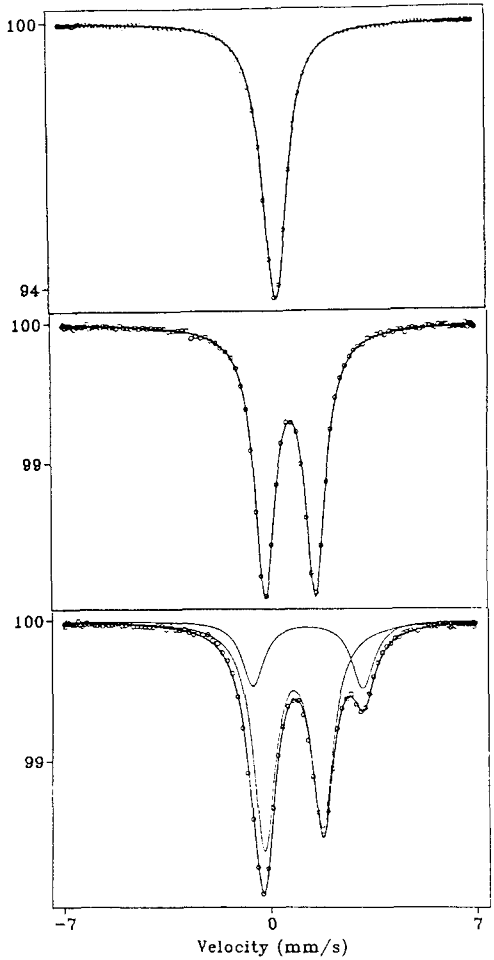

Fig. 3. Mössbauer spectra at 4.2 K of $SnCl_3(3\text{-}Me\text{-}pz)_3BH$, $CH_3SnCl_2(3\text{-}Me\text{-}pz)_3BH$ and $(CH_2{=}CH)_2(3\text{-}Me\text{-}pz)_2BH$ (from top to bottom) (experimental points: discontinuous curve drawn with small circles; fitted spectrum and relative components: continuous line).

The compounds have relatively low melting points, and also a Lamb–Mössbauer factor too small for observation of the Mössbauer effect at room temperature. This implies a rapid decrease in the strength of intermolecular forces with increasing temperature, and might be an indication that the structures in solution are retained even in the solid state.

Octahedral coordination, more or less distorted, is present in all the compounds of Table 9.

^{119}Sn-NMR and concluding remarks

^{119}Sn-NMR data are reported in Table 4; as found previously [3a], the chemical shift of tin varies with the electron donor ability of the substituents and the type of the ligand. Linear correlations are obtained for plots of chemical shift against the number of methyl (or butyl) groups attached to tin for each of the ligands L^B, L^0,

L^1 or L^2. In the case of phenyl derivatives, linearity is less evident and the slopes are less.

The more methyl groups in the pyrazole rings the more negative the chemical shifts. The chemical shift becomes more negative as the number of chlorine atoms increases. This is remarkable because plots of the ^{119}Sn chemical shift of the organotin(IV) halides $(\text{organyl})_n\text{Sn(Hal)}_{4-n}$ fit U-shaped curves due to competing diamagnetic and paramagnetic terms [20]. In the present case, the correlations on changing an R group for a Cl hold not only for ^{119}Sn, but also for the ^{13}C chemical shifts of Sn-attached carbons. Moreover, on changing from sp^3- to sp^2-hybridised carbon atoms bonded to tin (which should give a more positive charge on tin), the relationship with ^{119}Sn chemical shift is maintained (compare **2** *vs.* **4** and **5** *vs.* **8** or **9**) and qualitatively follow the Mössbauer isomer shift data, as noted above. However, dependence of shift on ligand cannot always so early be rationalized in terms of charge. The ^{119}Sn-NMR chemical shift is also influenced by other factors, among which steric hindrance may be significant.

In order to achieve a better understanding of the overall donor ability of the trispyrazolylborato-ligands, other tin compounds are being prepared with different ring substitutions.

Experimental

Concentration of solutions was always carried out *in vacuo* (water aspirator). The samples were dried *in vacuo* till constant weight (20°C, *ca.* 0.1 torr). Carbon, hydrogen, and nitrogen analyses were carried out in our Department; molecular weight determinations were performed at Pascher Mikroanalytisches Laboratorium, Remagen, Germany. Infrared spectra were recorded from 4000 to 250 and from 4000 to 600 cm^{-1} on a Perkin–Elmer 457 instrument and 1600 Series FTIR instrument, respectively. ^{1}H-, ^{13}C- and ^{119}Sn-NMR spectra were recorded on a VX-300 spectrometers operating at room temperature (300 MHz for ^{1}H, 75 MHz for ^{13}C and 111.9 MHz for ^{119}Sn). The conductances of solutions were measured with a Crison CDTM 522 conductimeter at room temperature. Melting points were taken on a IA 8100 Electrothermal instrument.

*Potassium hydridotris(3-methyl-1*H*-pyrazol-1-yl)borate (KL^1).* A mixture of 32.8 g (0.4 moles) of 3-methylpyrazole and 5.4 g (0.1 moles) of potassium borohydride was heated with stirring in a 250 mL flask attached through an air condenser to a gas meter. When about 3 L of dihydrogen had been evolved, the oil bath was replaced with a heating mantle, and the temperature was raised gradually over 3 h and then held for 24–36 h at about 195°C until a total of 7.5 l (0.3 moles) of dihydrogen had been evolved. The melt was poured slowly into 80 mL of stirred hot xylene. The resulting mixture was stirred for 3–5 min and then filtered hot.

The solid was washed in n-hexane/diethyl ether and air-dried yielding ~ 20 g (68%), m.p. 252–254°C.

*Dichloro[hydrotris(3-methyl-1*H*-pyrazol-1-yl)borate]methyltin(IV)* *2*. A solution/suspension of trichloromethyltin(IV) (240 mg, 1 mmol) in dichloromethane (25 mL) was added to a stirred suspension of potassium hydridotris(3-methyl-1*H*-pyrazol-1-yl)borate (294 mg, 1 mmol) in the same solvent (25 mL). After some hours, the filtered solution was evaporated to dryness; the residue washed with light petroleum and acetone and was recrystallized from dichloromethane-diethyl ether. Compounds **2**–**9** were obtained similarly.

Suitable crystals of compound **4** were obtained by slow evaporation of a dichloromethane-diethyl ether solution at sub-ambient temperature.

Mössbauer measurements

The $Ca^{119m}SnO_3$ Mössbauer source and the absorbers, with an Sn content of about 15 mg/cm^2, were both kept at 4.2 K. A sinusoidal velocity waveform and an intrinsic germanium detector were used. The fitting procedure was performed using the MOS 90 program. Our data and the literature data were compared without SOD shift correction. The width of the Mössbauer lines reported in Table 9 is close to the minimum observable width of 0.63 mm/s for ^{119m}Sn [19]. The area ratio between the two components of the doublet in some derivatives (**1**, **2** and **9** in Table 9) deviates from unity, possibly due to Goldanskii–Karyagin asymmetry.

X-Ray analysis

A crystal of dimension 0.10 × 0.28 × 0.28 mm was mounted on an Enraf-Nonius CAD4 diffractometer with graphite monochromated Mo-K_α radiation. The SEARCH program was used to obtain 25 reflections, which were used in the program INDEX to derive approximate cell dimensions. Accurate lattice parameters were obtained by least-squares refinement of these reflections. The monoclinic (C-centred) cell quoted was confirmed by the use of the TRACER program [21].

A total of 4679 independent reflections ($2 < \vartheta < 30°$) was measured at room temperature using the $\omega/2\vartheta$ scan. The intensities of three standard reflections were monitored every 300 min and showed no significant variation. A total of 3723 reflections with $I > 3\sigma(I)$ were regarded as observed. The intensities were corrected for Lorentz and polarization effects and for absorption according to North *et al.* [22] with minimum and maximum absorption factors of 0.9397 and 0.9988. An approximate absolute scale and a mean thermal factor of 2.12 Å^2 were determined by Wilson's method [23].

Structure determination and refinement

Systematic absences $h0l$, l odd and $h\ k\ l$, $h + k$ odd indicate the possible space groups $C2/c$ or C/c. The presence of strong $x0z$ vectors in the Patterson map agrees with the centrosymmetric group $C2/c$. The position of the tin atom was derived from the three-dimensional Patterson map. A difference electron density synthesis based upon the Sn signs revealed all the nonhydrogen atoms. The positions of the hydrogen atoms were calculated from the geometry of the compound and checked on a final difference Fourier map. The full-matrix least-squares anisotropic refinement, including the hydrogen atoms in fixed positions with the same isotropic thermal parameters as their bonded atoms gave an R factor of 0.054 ($R_w = 0.068$). The observed reflections were given unit weight. Weights obtained from counting statistics did not lead to better results. The final difference Fourier map showed maximum and minimum $\Delta\rho$ values 0.0613 and 0.0621 eÅ^{-3}, both of them close to the Sn atom.

All calculations were carried out with the Enraf-Nonius SDP crystallographic computing package [24] and with local programs.

Supplementary material available. Tables of thermal parameters, position of hydrogen atoms, planarity of molecular regions and a list of structure factors can be obtained from B. B. on request.

Acknowledgments

Financial support from the Consiglio Nazionale delle Ricerche (Roma), MURST, and NATO (CRG 920179 to S.C.) is gratefully acknowledged. The authors thank Fabio Marchetti (University of Camerino) and Giorgio Martorana (University of Venice) for technical assistance.

References

1 (a) J.R. Masaguer, E. Freijanes, J. Sordo, J.S. Casas and M.R. Bernejo, Inorg. Chim. Acta, 25 (1977) 203; (b) A.H. Cowley, C.J. Carrano, R.L. Geerts, R.A. Jones and C.M. Nunn, Angew. Chem., Int. Ed. Engl., 27 (1988) 277; (c) S. Trofimenko, J.C. Calabrese and J.S. Thompson, Angew. Chem., Int. Ed. Engl., 28 (1989) 205; (d) M.A.J. Moss and C.J. Jones, Polyhedron, 9 (1990) 1119; (e) A. Looney, Polyhedron, 9 (1990) 265; (f) K.B. Shiu, K.S. Liou, S.L. Wang and S.C. Wes, Organometallics, 9 (1990) 669; g) G. Gioia Lobbia, F. Bonati, P. Cecchi and C. Pettinari, Gazz. Chim. Ital., 121 (1991) 355.
2 (a) D.L. Reger, S.J. Knox, M.F. Huff, A.L. Rheigold and B.S. Haggerty, Inorg. Chem., 30 (1991) 1754; (b) M.N. Hansen, K. Niedenzu, J. Serwatowska, J. Servatowski and K. Woodrum, Inorg. Chem., 30 (1991) 866; (c) D.L. Reger, S.J. Knox, A.L. Rheigold and B.S. Haggerty, Organometallics, 9 (1990) 2581; (d) D.L. Reger, S.J. Knox and L. Lebioda, Organometallics, 9 (1990) 2218; (e) M. Di Vaira and F. Mani, J. Chem. Soc., Dalton Trans., (1990) 191; (f) S. Trofimenko, J.C. Calabrese, P.J. Domaille and J.S. Thompson, Inorg. Chem., 28 (1989) 1091.
3 (a) G. Gioia Lobbia, F. Bonati, P. Cecchi, A. Lorenzotti and C. Pettinari, J. Organomet. Chem., 403 (1991) 317; (b) G. Gioia Lobbia, F. Bonati, P. Cecchi and D. Leonesi, J. Organomet. Chem., 391 (1990) 155; (c) G. Gioia Lobbia, F. Bonati, P. Cecchi, A. Cingolani and A. Lorenzotti, J. Organomet. Chem., 378 (1989) 139.
4 C.K. Johnson, ORTEP, Report ORNL-3793, Oak Ridge National Laboratory, Tennessee, USA, 1965.
5 G.A. Miller and E.O. Schlemper, Inorg. Chem., 12 (1973) 677.
6 G. Poli, C.J. Cheer and W.H. Nelson, J. Organomet. Chem., 306 (1986) 347.
7 C. Pettinari, G. Rafaiani, G. Gioia Lobbia, A. Lorenzotti, F. Bonati and B. Bovio, J. Organomet. Chem., 405 (1991) 75.
8 B.K. Nicholson, J. Organomet. Chem., 265 (1984) 153.
9 O.S. Jung, J.H. Jeong and Y.S. Sohn, J. Organomet. Chem., 399 (1990) 235.
10 P.G. Harrison, T.J. King and J.A. Richards, J. Chem. Soc., Dalton Trans., (1976) 1414.
11 D. Searle, P.J. Smith, N.A. Bell, L.A. March, I.W. Nowell and J.D. Donaldson, Inorg. Chim. Acta, 162 (1989) 143.
12 C. Sreelatha, D.K. Srivastava, V.D. Gupta and H. Noeth, J. Chem. Soc., Dalton Trans., (1988) 407.
13 S. Calogero, G. Valle, P.A. Cusack, P.J. Smith and J.D. Donaldson, Inorg. Chim. Acta, 67 (1982) 95.
14 H. Koepf and P. Koepf-Maier, in S.J. Lippard (Ed.), Platinum, Gold and Other Metal Chemotherapeutic Agents: Chemistry and Biochemistry, A.C.S. Symp. Ser., 209, A.C.S., Washington DC, 1983, Ch. 16, p. 315.
15 A.H. Cowley, R.L. Geerts, C.M. Nunn, C.J. Carrano, J. Organomet. Chem., 341 (1988) C27.
16 S. Trofimenko, J.C. Calabrese and J.S. Thompson, Inorg. Chem., 26 (1987) 1507.
17 R.H. Herber, in F.A. Cotton (Ed.), Progress in Inorganic Chemistry, Vol. 8, Interscience, New York, 1967, p. 1.
18 (a) R.V. Parish, in G.J. Long (Ed.), Mössbauer Spectroscopy Applied to Inorganic Chemistry, Vol. 1, Plenum Press, New York, 1984, p. 527; (b) S. Calogero, D.A. Clemente, V. Peruzzo and G. Tagliavini, J. Chem. Soc., Dalton Trans., (1979) 1172.
19 G.K. Shenoy and F.E. Wagner, Mössbauer Isomer Shifts, North Holland, Amsterdam, 1978.
20 P.G. Harrison, in P.G. Harrison (Ed.), Chemistry of Tin, Blacki, Glasgow, 1989, Chap. 3, pp. 74–78, and references cited therein.
21 S.L. Lawton and R.A. Jacobson, TRACER, a cell reduction program, Ames Laboratory, Iowa State University of Science and Technology, Ames, IA, 1965.
22 A.C.T. North, D.C. Phillips and F.C. Mathews, Acta Crystallogr., Sect. A, 24 (1968) 351.
23 A.J.C. Wilson, Nature, 150 (1942) 152.
24 B.A. Frenz and Associates Inc., College Station, TX 77840 and Enraf-Nonius, Delft 1985.